Experimental validation of textured sensing skin for fatigue crack monitoring

Liu, Han, Laflamme, Simon, Li, Jian, Bennett, Caroline, Collins, William, et al.

Han Liu, Simon Laflamme, Jian Li, Caroline Bennett, William Collins, Austin Downey, Hongki Jo, "Experimental validation of textured sensing skin for fatigue crack monitoring," Proc. SPIE 11591, Sensors and Smart Structures Technologies for Civil, Mechanical, and Aerospace Systems 2021, 115911R (22 March 2021); doi: 10.1117/12.2582592

SPIE.

Event: SPIE Smart Structures + Nondestructive Evaluation, 2021, Online Only

Experimental Validation of Textured Sensing Skin for Fatigue Crack Monitoring

Han Liu[a], Simon Laflamme[a b], Jian Li[c], Caroline Bennett[c], William Collins[c], Austin Downey[d], and Hongki Jo[e]

[a]Department of Civil, Construction and Environmental Engineering, Iowa State University, Ames, IA, USA
[b]Department of Electrical and Computer Engineering, Iowa State University, Ames, IA, USA
[c]Department of Civil, Environmental and Architectural Engineering, The University of Kansas, Lawrence, KS, USA
[d]Department of Mechanical Engineering, University of South Carolina, Columbia, SC, USA
[e]Department of Civil, Architectural Engineering and Mechanics, The University of Arizona, Tucson, AZ, USA

ABSTRACT

Automatic fatigue crack detection using commercial sensing technologies is difficult due to the highly localized nature of crack monitoring sensors and the randomness of crack initiation and propagation. The authors have previously proposed and demonstrated a novel sensing skin capable of fatigue crack detection, localization, and quantification. The technology is based on soft elastomeric capacitors (SECs) that constitute thin-film flexible strain sensors transducing strain into a measurable change in capacitance. Deployed in an array configuration, the SECs mimic biological skin, where local damage can be diagnosed over large surfaces. Recently, the authors have proposed a significantly improved version of the SEC, whereby the top surface of the sensor is corrugated in diverse non-auxetic and auxetic patterns. Laboratory investigations of non-auxetic patterns have shown that the use of corrugation can increase the sensor's gauge factor, linearity, and signal stability when compared to untextured sensors, while numerical analyses of auxetic patterns have shown their superiority over non-auxetic corrugations. In this paper, we experimentally study the use of corrugated SECs, in particular with grid, diagrid, reinforced diagrid, and re-entrant hexagonal honeycomb-type (auxetic) patterns as a significant improvement to the untextured SEC in monitoring fatigue cracks in steel specimens. Results show that the use of corrugation significantly improves sensing performance, with both the reinforced diagrid and auxetic patterns yielding best results in terms of signal linearity, sensitivity, and resolution, with the reinforced diagrid having the added advantage of a symmetric pattern that could facilitate field deployments.

Keywords: Fatigue crack, flexible strain gauge, soft sensor, structural health monitoring, sensing skin, auxetic, corrugation, capacitor

1. INTRODUCTION

Fatigue-induced cracks in structural steel components are one of the primary safety concerns for transportation infrastructure.[1] Their early detection is critical in enabling timely maintenance and repair actions in order to prevent excessive damage and catastrophic failure.[2] This is typically done through visual inspections, but the process is time consuming, labor intensive, and frequently inaccurate for early-stage damage.[3,4] Nondestructive evaluation (NDE) techniques, such as ultrasonic[5] and magnetic particle testing,[6] are suitable alternatives due to their enhanced accuracy. However the use of NDE requires trained agents, and can be expensive and time consuming.

A solution is to use structural health monitoring (SHM) technologies to continuously monitor for the presence of fatigue cracks. Of interest to this paper are strain-based methods, which are widely used for the monitoring

Further author information: (Send correspondence to H.L.)
H.L.: E-mail: liuhan@iastate.edu

Sensors and Smart Structures Technologies for Civil, Mechanical, and Aerospace Systems 2021, edited by Haiying Huang, Daniele Zonta, Zhongqing Su, Proc. of SPIE Vol. 11591, 115911R
 · doi: 10.1117/12.2582592

of fatigue cracks, because their signal can be directly linked to the damage's presence and severity.[7,8] However, a key limitation of conventional strain sensing is that the transducers are relatively small in size, which makes the detection of a new crack unlikely on a probabilistic perspective.[9] The development of a cost-effective dense sensor network could empower effective fatigue crack detection through wide surface coverage capability.

Recently, researchers have proposed large-area electronics (LAE) sensing solutions, which can be deployed as a sensor network to collect dense sets of local measurements, also known as sensing skin, therefore facilitating the detection task.[10,11] Specific examples of LAE developed for fatigue crack monitoring includes piezoelectric wafer active sensor networks,[12,13] strain sensing sheets[14,15] and carbon nanotube-based sensing skin.[16,17] The authors in[9] have also proposed sensing skin technology based on a network of soft elastomeric capacitor (SEC), with a notable dense sensor network application for diagnosis and assessment of distortion-induced fatigue cracks.[18]

The SEC technology is a parallel plate capacitor formed by drop casting a high-permittivity compliant dielectric and applying compliant electrodes onto both surfaces, yielding a flat sensor that can be adhered onto the monitored material using an epoxy. Recent discoveries on the SEC showed that texturing the dielectric layer through various corrugated surface patters yielded significant improvement in signal linearity stability, and resolution, attributable to a higher gauge factor resulting from lowering the sensor's transverse Poisson's ratio, and to higher mechanical stability from augmenting the in-plane stiffnesses.[19] This study was conducted experimentally on free-standing SEC specimens, and extended numerically to auxetic patterns in,[20] where these auxetic patterns exhibited better performance compared to the non-auxetic patterns evaluated in.[19]

In this paper, the use of textured SECs for detecting and quantifying fatigue cracks in steel specimens is studied. In particular, four different patterns were selected based on prior work,[20] consisting of a grid, a diagrid, a reinforced diagrid, and a re-entrant hexagonal honeycomb pattern. The study is conducted on compact tension, C(T), specimens subjected to a dynamic load designed to generate low-cycle fatigue cracks extending to large damage sizes, thus enabling the quantification of the SEC performance at detecting low-cycle fatigue cracks and quantifying different levels of damage.

The paper is organized as follows. Section 2 provides the background on textured SEC technology including the derivation of its electromechanimal model and a description of selected corrugated patterns. Section 3 describes the experimental methodology. Section 4 presents and discusses results from the experimental investigation. Section 5 concludes the paper.

2. BACKGROUND

The SEC is a parallel plate capacitor. Its fabrication process is discussed in details by Laflamme et al.[21] Briefly, its dielectric is formed by drop-casting a styrene-ethylene/butylene-styrene (SEBS)-titania solution, and the electrodes consist of a painted SEBS-carbon black solution. A textured SEC is fabricated by drop-casting the dielectric into a steel mold,[20] and painting the conductive paint onto the dried surfaces. Figure 1(a) shows the picture of an SEC with a re-entrant hexagonal honeycomb pattern. In what follows, the electromechanical model characterizing the texture SEC's electrical response to applied strain is derived, and the corrugated patterns selected for the study are presented.

2.1 Electromechanical Model

The sensing principle of the SEC sensor is based on a measurable change in capacitance arising from the change in its geometry provoked by strain. Assuming low measurement frequency ($< 1kHz$), the initial capacitance C of an SEC can be written

$$C = e_0 e_r \frac{A}{h} \tag{1}$$

where $e_0 = 8.854$ pF/m is the vacuum permittivity, e_r is the relative permittivity, h is the thickness of the dielectric, and A is the electrode area of length l and width d as annotated in Figure 1(b). By differentiating Eq. 1 and apply Hooke's Law under the assumption of plane stress, the electromechanical model for un-textured SEC is given by:

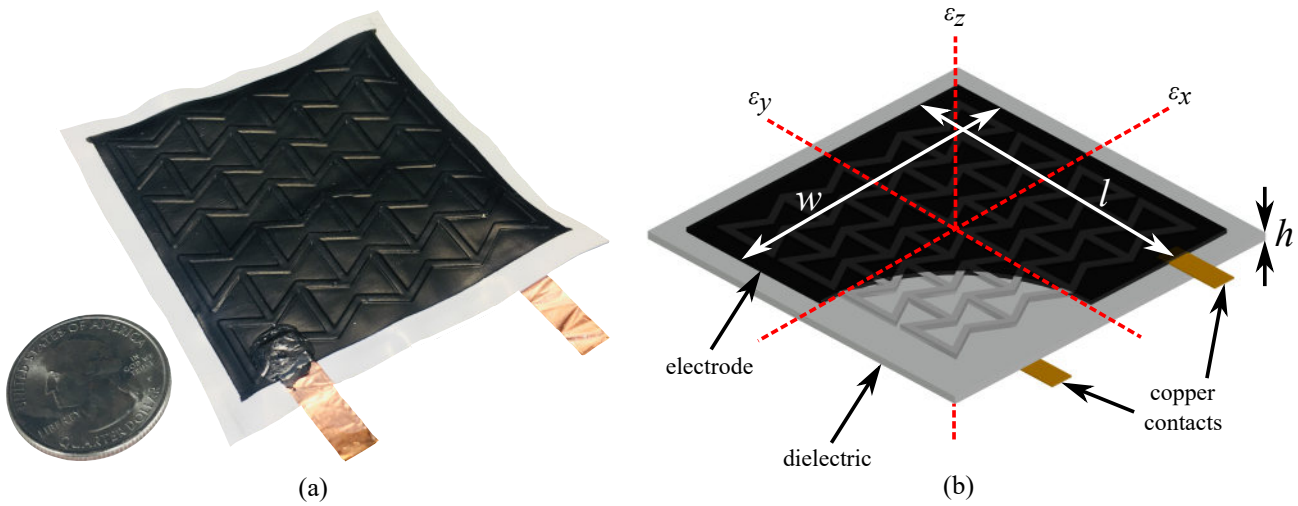

Figure 1. (a) Picture of a 76 mm × 76 mm textured SEC; and (b) annotated schematic of an SEC.

$$\frac{\Delta C}{C_0} = \frac{\nu}{1-\nu}(\varepsilon_x + \varepsilon_y) = \lambda(\varepsilon_x + \varepsilon_y) \tag{2}$$

where C_0 is the initial capacitance value, $\varepsilon_x = \Delta l/l$ and $\varepsilon_y = \Delta w/w$ are the in-plane strains. Textured patterns have stiffness diversity, thus the dielectric layer is treated as orthotropic in the $x-y$ plane. By assigning $\nu_{xy} = -\frac{\varepsilon_y}{\varepsilon_x}$ and substituting it into Eq. 2, the capacitance response of a free-standing textured SEC subjected to uniaxial strain (along the x direction) can be written as:

$$\frac{\Delta C}{C_0} = \left(\frac{1-\nu_{xy}}{1-\nu}\right)\varepsilon_x = \lambda\varepsilon_x \tag{3}$$

where $\nu = \nu_{xz} = \nu_{yz}$ is the Poisson's ratio in the $x-y$ and $x-z$ planes, and λ is the resulting gauge factor. Eq. 3 indicates that the gauge factor λ of a textured SEC varies as a function of the transverse Poisson's ratios, and increases with decreasing ν_{xy}. It follows that the gauge factor λ is also influenced by the stiffness of the monitored material and the level of sensor adhesion to the monitored surface. For simplicity, these factors are combined under the term $\nu_{xy,\mathbf{c}}$ denoting the transverse Poisson's ratio under composite effect, with Eq. 3 becoming

$$\lambda = \frac{1-\nu_{xy,\mathbf{c}}}{1-\nu} \tag{4}$$

2.2 Selected Corrugated Patterns

Based on results from prior work evaluating the performance of various non-auxetic[19] and auxetic[20] textures, four candidate corrugated patterns are selected: a symmetric diagonal grid, a diagrid, a reinforced diagrid, and a non-symmetric re-entrant hexagonal honeycomb pattern. The diagonal grid (Figure 2(a)) is selected because of its fabrication simplicity. The diagrid pattern (Figure 2(b)) is selected because it exhibited best performance among other non-auxetic patterns in,[19] while the reinforced diagrid pattern (Figure 2(c)) is selected to provide a symmetric option. The re-entrant hexagonal honeycomb pattern (Figure 2(d)) is an auxetic pattern, selected because it exhibited best performance among other auxetic patterns in.[20] Each corrugated pattern forms the top-surface texture of the sensing film with a sensing area of 63.5 mm by 63.5 mm (2.5 in by 2.5 in). The untextured pattern (flat pattern) used in prior work[9] is also considered in the evaluation for benchmarking purposes. Three SEC specimens are fabricated under each pattern, for a total of 15 samples.

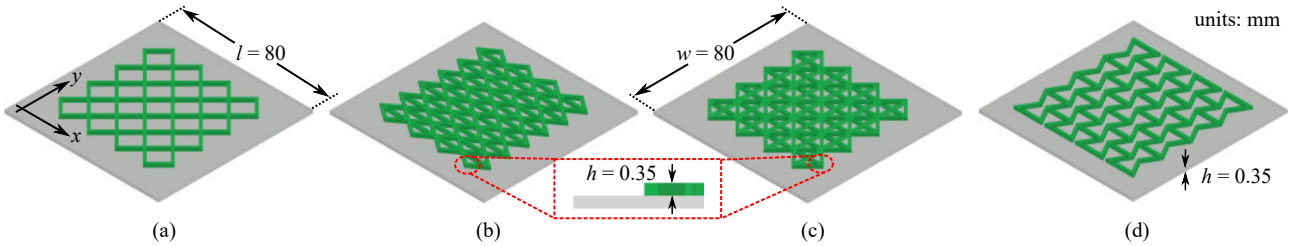

Figure 2. Evaluated corrugated patterns: (a) symmetric diagonal grid; (b) diagrid; (c) symmetric reinforced diagrid; and (d) re-entrant hexagonal honeycomb (auxetic) pattern.

3. EXPERIMENTAL METHODOLOGY

The performance of textured SECs at detecting and quantifying crack-type damage are evaluated on C(T) specimens following the procedure in Kong et al.[22] Figure 3 shows the experimental configuration. As observable in Figure 3(b), the SEC sample is fully adhered onto the frontside of the C(T) specimen, here using the off-the-shelf bi-component epoxy (JB Weld). For the non-symmetric patterns (diagrid and re-entrant hexagonal honeycomb patterns), the sensors are adhered such their $y-$ axis is aligned with the axial load and thus perpendicular to the fatigue crack in order to provide higher electrical sensitivity to damage. A measuring tape is adhered onto the backside of the C(T) specimen (Figure 3(c)) to quantify the length of the crack through pictures taken during the test. The SEC-C(T) specimen is connected to a pair of clevises mounted onto a servo-hydraulic testing machine (MTS model 312.41 with a TestStar IIm controller), and washers are used in conjunction with the screw nut to prevent relative sliding and distribute stress evenly.

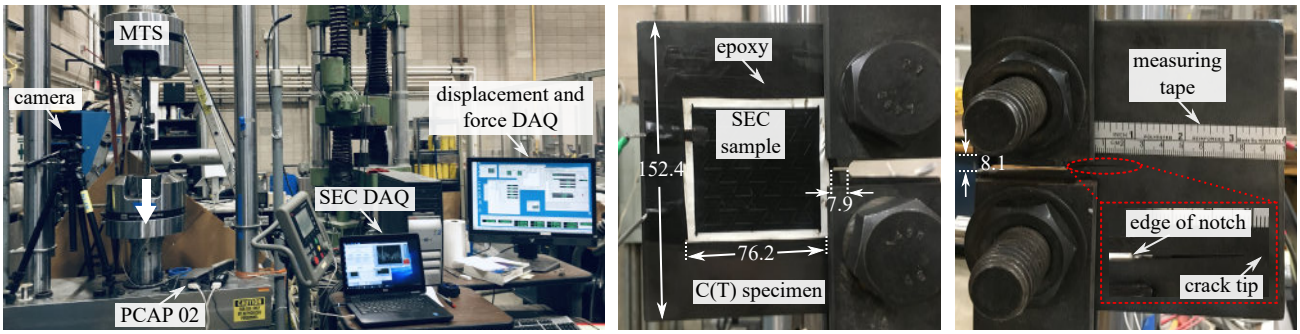

Figure 3. (a) Experimental configuration (arrow indicates the loading direction); (b) zoom on the front side of SEC-C(T) specimen; and (c) zoom on the back side of SEC-C(T) specimen. Units: mm

A 2 Hz harmonic excitation is applied to the specimen, and the loading range is assigned in the tension-tension mode between 2.9 kN (0.65 kips) and 29 kN (6.5 kips) to generate and extend a fatigue crack. Remark that this load intensity is higher than prescribed in ASTM E647-15a in order to accelerate the crack growth and enable the quantification of the SEC performance at both detecting low-cycle fatigue cracks and quantifying different levels of damage. Load and displacement values are recorded at a 20 Hz sampling rate. Capacitance data is collected using an off-the-shelf data acquisition board (ACAM PCAP02) at a 25 Hz sampling rate. Wires are fixed with black tapes for minimizing electrical noise. Figure 3(c) shows a fatigue crack that was generated during a typical test. The crack length is taken as the distance measured between the tip of the crack and the edge of the notch.

4. RESULTS AND DISCUSSION

Figure 4(a) shows a typical capacitance and strain input signal time series, exhibiting good agreement between both signals. In analysing the performance of the various textured SECs, the average peak-to-peak (P2P) over different crack lengths is extracted. This strategy allows for the filtering of signal drifts due to calibration

and environmental effects. Figure 4(a) also shows a bar chart that compares the P2P relative capacitance amplitudes under each pattern over the different crack lengths. It is found that the use of corrugated surfaces significantly improves the sensitivity of the signal to damage, attributable to a higher gauge factor. Textured SECs yield an average 53.2% (at 21.6 mm) to 106.1% (at 17.5 mm) increase in P2P amplitude with respect to the untextured SEC. A cross-comparison between patterns shows that the reinforced diagrid ('reinforced') and the re-entrant hexagonal honeycomb ('auxetic'. see the reinforced word above) patterns generally outperforms all other patterns, with the reinforced diagrid pattern showing better performance over larger crack sizes.

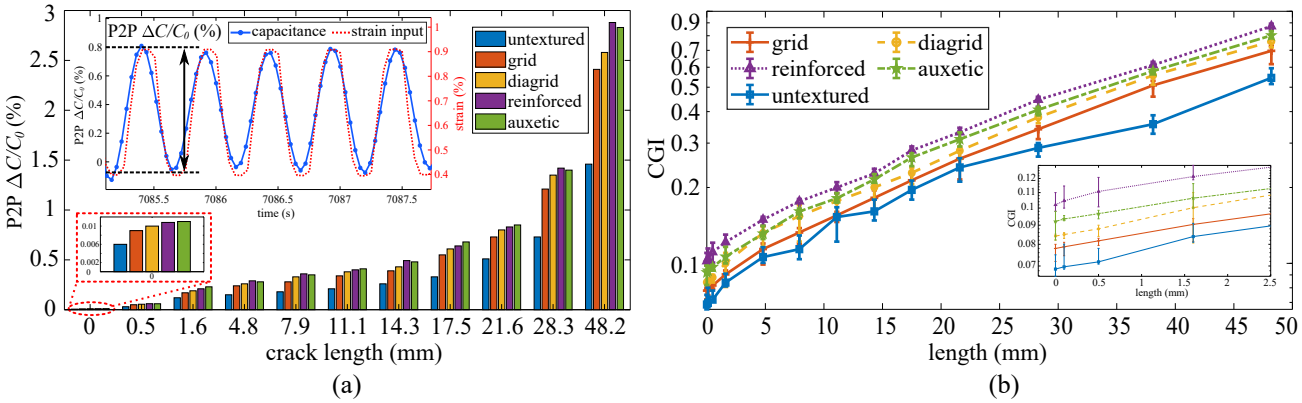

Figure 4. (a) P2P amplitudes of the relative change in capacitance $\Delta C/C_0$ under all patterns over different crack lengths; and (b) semi-log plot of CGI as a function of crack length under all patterns.

Table 1. Experimental results from the studied signals.

pattern	crack length (mm)	MTS strain (−)	R^2 (−)	λ (−)	95% CI fit $\Delta C/C_0$ (−)	resolution ($\mu\varepsilon$)
grid	0	0.39	0.13	0.065	±0.76	±1169
diagrid	0	0.39	0.15	0.073	±0.69	±945
reinforced	0	0.39	0.14	0.086	±0.63	±741
auxetic	0	0.39	0.17	0.082	±0.59	±719
untextured	0	0.39	0.08	0.051	±1.18	±2314
grid	11.1	0.73	0.77	0.49	±0.36	±73.4
diagrid	11.1	0.73	0.79	0.51	±0.38	±74.5
reinforced	11.1	0.73	0.74	0.57	±0.31	±54.4
auxetic	11.1	0.73	0.83	0.59	±0.29	±49.2
untextured	11.1	0.73	0.46	0.33	±0.61	±184
grid	48.2	1.62	0.95	1.53	±0.31	±20.3
diagrid	48.2	1.62	0.96	1.65	±0.29	±17.5
reinforced	48.2	1.62	0.93	1.92	±0.27	±14.1
auxetic	48.2	1.62	0.97	1.88	±0.23	±12.2
untextured	48.2	1.62	0.72	0.96	±0.49	±51.1

Figure 4(b) fuses results in term of the crack growth index (CGI) proposed in Kong et al.,[23] where the CGI is plotted as the average over the three specimens along with the associated min-max values bar. The CGI is taken as the square root of the ratio of the magnitude of the frequency peak of the signal to the magnitude of the frequency peak of the input. A linear relationship between the log CGI and the crack length is desirable to obtain an actionable metric. It can be observed that the use of a corrugated pattern significantly increases the linearity of the CGI with respect to the untextured configuration, with the linear fit coefficients of determination (R^2) being 0.948 (grid), 0.952 (diagrid), 0.971 (reinforced diagrid), 0.963 (auxetic), and 0.912 (untextured). The reinforced diagrid pattern outperformed all other patterns and showed slightly more linear compared to the

auxetic pattern.

Table 1 quantifies the quality of the time series signals over three representative crack lengths: 0, 11.1, and 48.2 mm. It tabulates the linearity (quality of linear fit capacitance-to-strain, R^2) along with the relative sensitivity (gauge factor λ) and resolution (95% confidence interval). The strain level for the 95% fit was computed using Equation 4 with the reported λ. Results show that the use of corrugated patterns clearly improves performance in terms of linearity, sensitive, and resolution over all crack lengths, compared against the untextured SEC. The auxetic pattern exhibits the best performance in terms of the linearity and resolution, yielding between 34.7% and 112.5% increase in R^2 and between 221.8% and 318.8% improvement in resolution with respect to the untextured sensor. The reinforced pattern generally exhibits the best performance in terms of sensitivity, with an increase in gauge factor λ between 68.6% and 99.8% with respect to the untextured SECs, consistent with results from the P2P investigation. Remark that the textured SEC offers a poor resolution for the 0 mm crack length.

5. CONCLUSION

This paper presented a study on the performance of a textured soft elastomeric capacitor (SEC) for the detection and quantification of fatigue cracks. Specifically, four corrugated patterns were studied: a grid, a diagrid, a reinforced diagrid, and a re-entrant hexagonal honeycomb pattern. Results were benchmarked against those obtained using an untextured SEC, used for the same purpose in prior work.

The study was conducted by adhering SECs onto compact tension, C(T), specimens subjected to a cyclic load designed to generate low-cycle fatigue cracks extending to large crack length and opening, thus enabling the quantification of the SEC performance at detecting low-cycle fatigue cracks and quantifying different levels of damage. Compared against the untextured SEC, results showed that the use of a corrugated pattern significantly improved on the linearity crack growth index (CGI), a previous developed crack quantification metric, and also improved the signal in terms of linearity, sensitivity, and resolution. A cross-comparison between the various patterns showed that both the reinforced diagrid and the re-entrant hexagonal honeycomb (auxetic) patterns yielded the best performance.

The presented corrugated sensor is thus a considerable improvement with respect to the untextured sensor for field applications. The reinforced diagrid offer a significant advantage over the auxetic pattern through its symmetry, resulting in a much simplified deployment. Future work is to further study the quality of the SEC signals over more complex geometries, and to evaluate its performance in the field.

ACKNOWLEDGMENTS

The authors would like to gratefully acknowledge the financial support of Iowa State University and the University of Iowa through the joint seed grant program, and of the Departments of Transportation of Iowa, Kansas, South Carolina, and North Carolina, through the Transportation Pooled Fund Study TPF-5(449). The authors are also grateful to Douglas Wood at Iowa State University for his assistance with tests.

REFERENCES

[1] Campbell, F., ed., [Fatigue and Fracture: Understanding the Basics], ASM International (2012).

[2] Haghani, R., Al-Emrani, M., and Heshmati, M., "Fatigue-prone details in steel bridges," Buildings **2**, 456–476 (nov 2012).

[3] Campbell, L. E., Connor, R. J., Whitehead, J. M., and Washer, G. A., "Human factors affecting visual inspection of fatigue cracking in steel bridges," Structure and Infrastructure Engineering , 1–12 (sep 2020).

[4] Yao, Y., Tung, S.-T. E., and Glisic, B., "Crack detection and characterization techniques-an overview," Structural Control and Health Monitoring **21**, 1387–1413 (mar 2014).

[5] Liu, P., Lim, H. J., Yang, S., Sohn, H., Lee, C. H., Yi, Y., Kim, D., Jung, J., and hwan Bae, I., "Development of a "stick-and-detect" wireless sensor node for fatigue crack detection," Structural Health Monitoring: An International Journal **16**, 153–163 (sep 2016).

[6] Zolfaghari, A., Zolfaghari, A., and Kolahan, F., "Reliability and sensitivity of magnetic particle non-destructive testing in detecting the surface cracks of welded components," Nondestructive Testing and Evaluation **33**, 290–300 (jan 2018).

[7] Burton, A. R., Lynch, J. P., Kurata, M., and Law, K. H., "Fully integrated carbon nanotube composite thin film strain sensors on flexible substrates for structural health monitoring," Smart Materials and Structures **26**, 095052 (aug 2017).

[8] Zhang, B., Zhou, Z., Zhang, K., Yan, G., and Xu, Z., "Sensitive skin and the relative sensing system for real-time surface monitoring of crack in civil infrastructure," Journal of Intelligent Material Systems and Structures **17**, 907–917 (oct 2006).

[9] Kharroub, S., Laflamme, S., Song, C., Qiao, D., Phares, B., and Li, J., "Smart sensing skin for detection and localization of fatigue cracks," Smart Materials and Structures **24**, 065004 (may 2015).

[10] Liao, X., Liao, Q., Yan, X., Liang, Q., Si, H., Li, M., Wu, H., Cao, S., and Zhang, Y., "Flexible and highly sensitive strain sensors fabricated by pencil drawn for wearable monitor," Advanced Functional Materials **25**, 2395–2401 (mar 2015).

[11] Wang, Y., Qiu, L., Luo, Y., and Ding, R., "A stretchable and large-scale guided wave sensor network for aircraft smart skin of structural health monitoring," Structural Health Monitoring , 147592171985064 (jun 2019).

[12] Zhou, C., Hong, M., Su, Z., Wang, Q., and Cheng, L., "Evaluation of fatigue cracks using nonlinearities of acousto-ultrasonic waves acquired by an active sensor network," Smart Materials and Structures **22**, 015018 (dec 2012).

[13] M. Gresil, L. Yu, Y. S. and Giurgiutiu., V., "Predictive model of fatigue crack detection in thick bridge steel structures with piezoelectric wafer active sensors," Smart Structures and Systems (2013).

[14] Yao, Y. and Glisic, B., "Detection of steel fatigue cracks with strain sensing sheets based on large area electronics," Sensors **15**, 8088–8108 (apr 2015).

[15] Glisic, B., Yao, Y., Tung, S.-T. E., Wagner, S., Sturm, J. C., and Verma, N., "Strain sensing sheets for structural health monitoring based on large-area electronics and integrated circuits," Proceedings of the IEEE **104**, 1513–1528 (aug 2016).

[16] Sánchez-Romate, X. F., Sbarufatti, C., Sánchez, M., Bernasconi, A., Scaccabarozzi, D., Libonati, F., Cinquemani, S., Güemes, A., and Ureña, A., "Fatigue crack growth identification in bonded joints by using carbon nanotube doped adhesive films," Smart Materials and Structures **29**, 035032 (feb 2020).

[17] Ahmed, S., Schumacher, T., Thostenson, E. T., and McConnell, J., "Performance evaluation of a carbon nanotube sensor for fatigue crack monitoring of metal structures," Sensors **20**, 4383 (aug 2020).

[18] Kong, X., Li, J., Collins, W., Bennett, C., Laflamme, S., and Jo, H., "Sensing distortion-induced fatigue cracks in steel bridges with capacitive skin sensor arrays," Smart Materials and Structures **27**, 115008 (oct 2018).

[19] Liu, H., Yan, J., Kollosche, M., Bentil, S. A., and Laflamme, S., "Surface textures for stretchable capacitive strain sensors," Smart Materials and Structures **29**, 105037 (sep 2020).

[20] Liu, H., Kollosche, M., Yan, J., Zellner, E. M., Bentil, S. A., Rivero, I. V., Wiersema, C., and Laflamme, S., "Numerical investigation of auxetic textured soft strain gauge for monitoring animal skin," Sensors **20**, 4185 (jul 2020).

[21] Laflamme, S., Saleem, H. S., Vasan, B. K., Geiger, R. L., Chen, D., Kessler, M. R., and Rajan, K., "Soft elastomeric capacitor network for strain sensing over large surfaces," IEEE/ASME Transactions on Mechatronics **18**, 1647–1654 (dec 2013).

[22] Kong, X., Li, J., Bennett, C., Collins, W., and Laflamme, S., "Numerical simulation and experimental validation of a large-area capacitive strain sensor for fatigue crack monitoring," Measurement Science and Technology **27**, 124009 (oct 2016).

[23] Kong, X., Li, J., Collins, W., Bennett, C., Laflamme, S., and Jo, H., "A large-area strain sensing technology for monitoring fatigue cracks in steel bridges," Smart Materials and Structures **26**, 085024 (jul 2017).